数理解析研究所講究録 1234 巻 2001 年 127-145

Comparison between the Boussinesq and coupled Euler equations in two dimensions

Koji Ohkitani

Research Institute for Mathematical Sciences,
Kyoto University
ohkitani@kurims.kyoto-u.ac.jp

Dedicated to the memory of the late Professor Tosio Kato

Abstract

A method of successive approximations is proposed for constructing a solution of the ideal two-dimensional Boussinesq equations on the basis of those of Euler equations. Numerical experiments on the iteration scheme suggest that the coupled Euler equations approximate the Boussinesq equations fairly well at the fifth iteration. The fast convergence of the successive approximations is consistent with global regularity of the Boussinesq equations, as long as the current numerical results are concerned. This method will serve as a solid check in monitoring a possible singularity formation numerically at much higher spatial resolutions.

1 Introduction

In 1964 Professor Tosio Kato published an elegant paper [1] on the global regularity of the two-dimensional Euler equations subject to a smooth external forcing

$$\frac{\partial \boldsymbol{u}}{\partial t} + (\boldsymbol{u}\cdot\nabla)\boldsymbol{u} = -\nabla p + \boldsymbol{f}, \tag{1}$$

$$\nabla\cdot\boldsymbol{f} = 0. \tag{2}$$

Here $\boldsymbol{u}$ and p denote the velocity and the pressure and $\boldsymbol{f}$ is an external forcing which may depend on space and time. The incompressibility condition determines the pressure and it has the following integral representation in $\mathbb{R}^2$

$$p = \frac{-1}{2\pi}\int_{\mathbb{R}^2} \frac{\partial u_i(\boldsymbol{y})}{\partial y_j}\frac{\partial u_j(\boldsymbol{y})}{\partial y_i}\log|\boldsymbol{x}-\boldsymbol{y}|d\boldsymbol{y}, \tag{3}$$

which can be obtained by solving

$$\triangle p = -\frac{\partial u_i}{\partial x_j}\frac{\partial u_j}{\partial x_i}. \tag{4}$$

The vorticity $\omega = \partial_1 u_2 - \partial_2 u_1$ obeys

$$\frac{\partial \omega}{\partial t} + (\boldsymbol{u}\cdot\nabla)\omega = \partial_1 f_2 - \partial_2 f_1. \tag{5}$$

While the vorticity is not conserved because of the forcing term, it is nevertheless well controlled if the forcing term is assumed to be sufficiently smooth. An account of the papers on the two-dimensional Euler equations can be found in [2], where

[3], [4] are surveyed. See also the unpublished manuscript [5] contained in this volume. All the four papers have used successive approximations to construct classical solutions of the two-dimensional Euler equations. To prove convergence of successive approximations, different methods have been employed, that is, Ascoli-Arzela's theorem was used in [3], a more direct proof by mathematical induction in [4] and Schauder's fixed point theorem in [1], [5].

In contrast to the case of Euler equations, the question whether solutions to the ideal Boussinesq equations with neither viscosity nor thermal conductivity, develop spontaneous singularity is an open problem, which has been controversial, not only theoretically but also numerically. In this paper in order to shed some light on this unsolved problem, we compare the ideal Boussinesq equations with the coupled two-dimensional Euler equations, the latter of which are known to have global smooth solutions.

The two-dimensional Boussinesq equations can be written as

$$\frac{\partial \boldsymbol{u}}{\partial t} + (\boldsymbol{u}\cdot\nabla)\boldsymbol{u} = -\nabla q + \begin{pmatrix} 0 \\ \theta \end{pmatrix}, \tag{6}$$

$$\nabla\cdot\boldsymbol{u} = 0, \tag{7}$$

and the temperature θ is conserved

$$\frac{\partial \theta}{\partial t} + (\boldsymbol{u}\cdot\nabla)\theta = 0, \tag{8}$$

where we have used a notation q for the pressure. The initial data $\omega(0)$ and $\theta(0)$ are assumed to be smooth. It should be noted that the second term on the right-hand side of (6) is not divergence-free (see Section 4.2).

The two-dimensional Boussinesq equations can be written in vorticity form as

$$\frac{\partial \omega}{\partial t} + (\boldsymbol{u}\cdot\nabla)\omega = \frac{\partial \theta}{\partial x_1}. \tag{9}$$

The vorticity is not conserved because of the presence of the temperature gradient in a troublesome way. Needless to mention, it is not possible to regard this term as a smooth external forcing because the temperature not only affects the flow field but also it is influenced by the flow field. That is, there is a closed loop of linkage in the interaction between the variables ω and θ. Because of this feedback mechanism the temperature gradient is out of control under time evolution. Other basic properties of the two-dimensional Boussinesq equations are summarized in the Appendices.

Indeed, it has been proved in [6],[7] that the maximum norm of $|\nabla\theta|$ controls regularity of (9) in the same spirit of a cerebrated theorem established for the three-dimensional Euler equations [8]. A number of numerical simulations have been conducted for (6) (or, for analogous three-dimensional axisymmetric Euler equations, see Appendix 6.3) [9]-[14]. Some of them indicated blow-up in finite time. But there is no proof that shows breakdown of smooth solutions for (9), that is, not a single analytic example is known that blows up in finite time.

2 Successive approximations

We show how we can construct solutions of the Boussinesq equations on the basis of the solutions of the Euler equations by successive approximations. That way we

can assess clearly the similarity and difference between solutions of the Boussinesq and Euler equations.[1]

2.1 The kick-and-advect formalism

Suppose we compare (8) and (9) with

$$\frac{\partial \omega^0}{\partial t} + (\boldsymbol{u}^0 \cdot \nabla)\omega^0 = 0, \tag{10}$$

$$\frac{\partial \theta^0}{\partial t} + (\boldsymbol{u}^0 \cdot \nabla)\theta^0 = 0. \tag{11}$$

The above set of equations is just a two-dimensional Euler flow and a passive scalar advected by it. If the initial conditions are regular, both ω^0 and θ^0 remain so for all time. Therefore $\nabla\theta^0$ may grow in time but never becomes unbounded in finite time. We thus expect that growth of $\nabla\theta^0$ is much weaker than that of $\nabla\theta$.

Then, regard $\nabla\theta^0$ as a forcing term and consider yet another two-dimensional Euler flow of the form (the kick stage)

$$\frac{\partial \omega^1}{\partial t} + (\boldsymbol{u}^1 \cdot \nabla)\omega^1 = \frac{\partial \theta^0}{\partial x_1}. \tag{12}$$

Since θ^0 is smooth all the time, we may apply the globally existence theorem of forced two-dimensional Euler equations to deduce that $\boldsymbol{u}^1$ is smooth all the time. Then the passive scalar θ^1 advected by it (the advect stage) as

$$\frac{\partial \theta^1}{\partial t} + (\boldsymbol{u}^1 \cdot \nabla)\theta^1 = 0 \tag{13}$$

remain regular for all time. We may repeat this argument as many times as we wish.

2.2 Coupled Euler equations

The above argument suggests how we may construct 'less regular' solutions of forced Euler equations in an iterative manner. Thus, in general we are led to compare (7)-(9) with a coupled system of two-dimensional Euler equations of the following form

$$\frac{\partial \omega^n}{\partial t} + (\boldsymbol{u}^n \cdot \nabla)\omega^n = \frac{\partial \theta^{n-1}}{\partial x_1}, \tag{14}$$

$$\frac{\partial \theta^n}{\partial t} + (\boldsymbol{u}^n \cdot \nabla)\theta^n = 0, \tag{15}$$

$$\nabla \cdot \boldsymbol{u}^0 = \nabla \cdot \boldsymbol{u}^n = 0, \tag{16}$$

for $n = 0, 1, 2, \ldots N$ with

$$\theta^{-1} \equiv 0,$$

[1] A comparison to two-dimensional Euler equations of another kind of active scalar equations (surface quasigeostrophic equations) has been done in [15]. No successive approximations were not introduced in that case.

where the superscript n denotes the number of iterations. The initial data are taken to be

$$\omega^0(0) = \omega^n(0)$$

and

$$\theta^0(0) = \theta^n(0),$$

for $n = 1, 2, \ldots, N$. As noted above, the zero-th order solution (ω^0, θ^0) is a set of the solutions of the conventional two-dimensional Euler equations and a passive scalar advected by it.

While the system (14), (15) is big, i.e. made up of lots of equations, the interaction among the variables ω^n and θ^n is one-way and there is no closed loop in their linkage, in a marked contrast to (8), (9).

2.3 Some properties of the iteration scheme

It should be noted that there are two limiting processes involved in the problem: one is the limit of taking large iteration number $N \to \infty$ and the other one is the extension of the time interval $[0, T]$ over which smooth solutions exist. We note the following basic properties.

(i) For fixed N, the system (14)-(16) has global solutions, that is, smooth solutions persist on any time interval $[0, T]$, no matter how large T is ([1]).

(ii) For sufficiently large N, $(\boldsymbol{u}^N, \theta^N)$ is a good approximation to the Boussinesq equations, at least for short time development. If there is no blowup in finite time, we expect that this is true for arbitrarily large T.

(iii) If $(\boldsymbol{u}^N, \theta^N)$ has a limit in some sense as $N \to \infty$, that is, the system (14)-(16) has a kind of 'fixed-point property', it solves the Boussinesq equations. In this limit, the iteration scheme retrieves the closed interaction between the vorticity and the temperature. Below, numerical results will be presented in some detail regarding this issue.

3 Numerical experiments

3.1 Numerical Method

We assume periodic boundary conditions in $[0, 2\pi]^2$ for numerical experiments. We use a standard pseudo-spectral method for numerical solutions of (14)-(16) under periodic boundary conditions. The 2/3-rule is used for dealiasing and the maximum wavenumber retained is $M/3$ for calculations with M^2 grid points. We use $M = 512$ and 1024 for solving (14)- (16) with the iteration number $N = 10$. Time-marching is performed by a forth-order Runge-Kutta method. Two kinds of initial conditions are used.

3.2 Numerical results

The first initial condition IC1 is

$$\text{IC1} \quad \omega(\boldsymbol{x}, 0) = \theta(\boldsymbol{x}, 0) = \sin x \sin y + \cos y \tag{17}$$

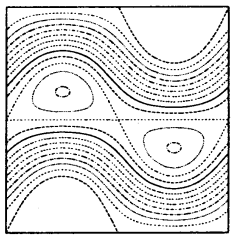

Fig.1: Contours of vorticity of IC1 in $[0, 2\pi]^2$. Contour levels are $\omega = -1.4, -1.2, -1.0, \ldots 1.4$.

whose contours are depicted in Fig.1. This is the initial condition used in a study on another kind of active scaler equation [16, 17].

The time evolution of contours of θ for IC1 is shown in Fig.2(a)-(e) for the iteration numbers $n = 0, 1, 2, 5$ and ∞. In the Euler case $n = 0$ (Fig.2(a)), there is a rotational symmetry around a point (π, π) which is preserved under the Eulerian dynamics (Fig.2(a)). For $n = 1$ such a symmetry is broken (Fig.2(b)) and the pattern is markedly different from that of $n = 0$. The difference between $n = 1$ and $n = 2$ (Fig.2(c)) is noticeable but not very large. The difference between $n = 2$ and $n = 5$ (Fig.2(d)) is even smaller. It should be noted that the pattern for $n = 5$ is virtually indistinguishable from that of the Boussinesq case $n = \infty$ (Fig.2(e)).

To quantify the above similarity between the Boussinesq and Euler equations we show in Fig.3(a) the normalized correlation coefficient $C(\theta^n, \theta^\infty)$ between θ^n and θ^∞ for $n = 0, 1, 2, 3, 4$ and 5. It is defined by

$$C(\theta^n, \theta^\infty) = \frac{\langle \theta^n \theta^\infty \rangle}{\sqrt{\langle (\theta^n)^2 \rangle \langle (\theta^\infty)^2 \rangle}}.$$

The correlation coefficients is 1 initially because the two fields are identical by definition. As expected, the correlation between $n = 0$ (Euler) and $n = \infty$(Boussinesq) decays quite quickly. Naturally, the time interval over which the correlation remains close to unity extends as n increases. However, it should be noted that at the iteration $n = 5$ the correlation survives fairly well, e.g., $C(\theta^5, \theta^\infty) = 0.99997$ at $t = 4.0$. Note that $t = 4$ is the maximal time when the flow is resolved accurately and is not to be considered as 'short'. This substantiates the observation made in Fig.2(d) and (e) that at the iteration number $n = 5$ the contours are indistinguishable between the coupled Euler and Boussinesq equations. A similar coefficient $C(\omega^n, \omega^\infty)$ between ω^n and ω^∞ is plotted in Fig.3(b). Again, at $n = 5$ the correlation coefficient remains close to unity up to $t = 5$.

Next, we compare the growth of the passive scalar gradient with that of the temperature gradient. In Fig.4(a) we show the time evolution of the spatial averages of squared gradient of θ^n

$$P_n(t) = \frac{1}{2} \langle |\nabla \theta^n|^2 \rangle,$$

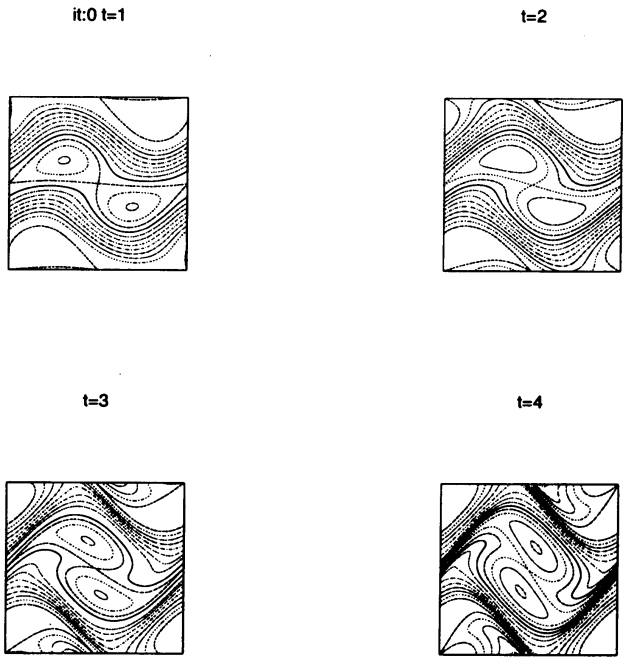

Fig.2(a): Time evolution of contours of the temperature for $n = 0$(the Euler case), depicted as in Fig.1

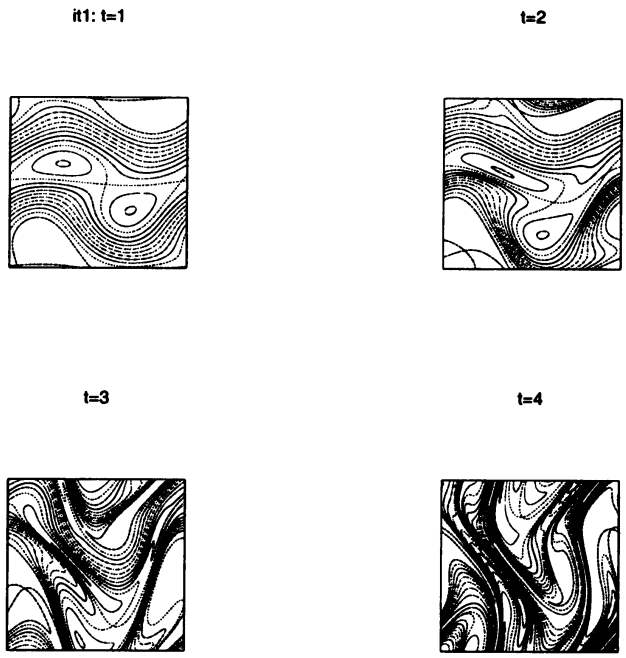

Fig.2(b): Time evolution of contours of the temperature for $n = 1$.

133

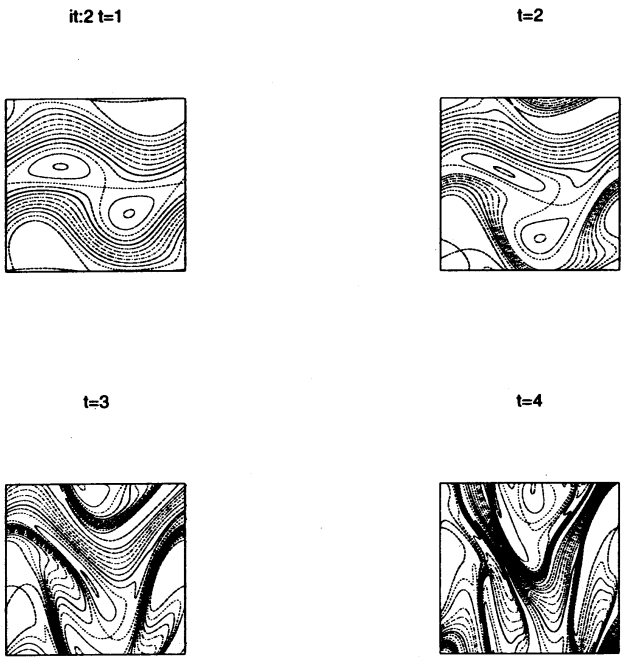

Fig.2(c): Time evolution of contours of the temperature for $n = 2$.

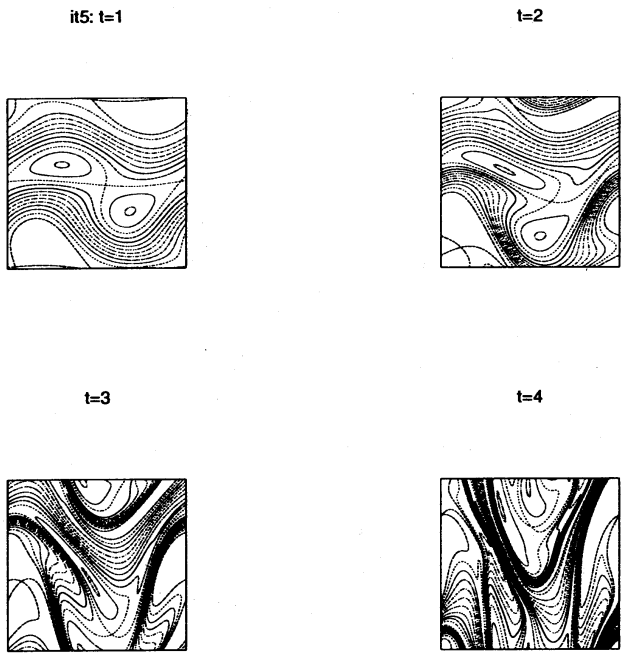

Fig.2(d): Time evolution of contours of the temperature for $n = 5$.

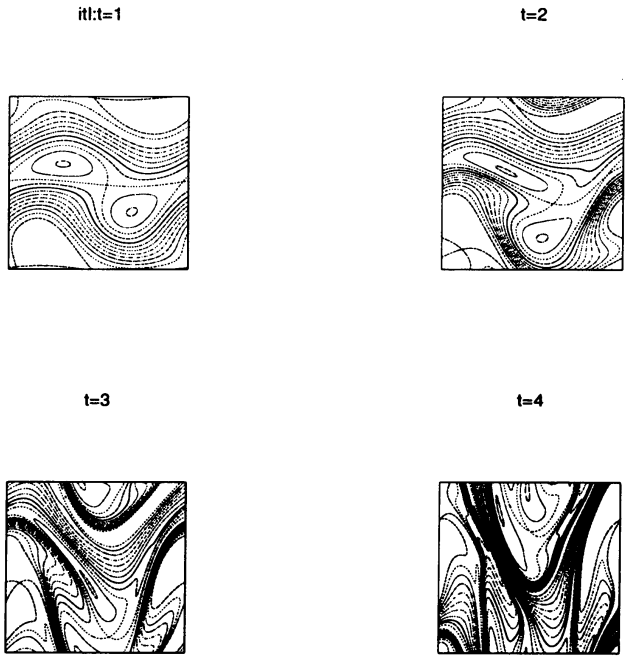

Fig.2(e): Time evolution of contours of the temperature for $n = \infty$ (the Boussinesq case).

for $n = 0, 1, 2, 5$ and ∞. All the norms show slightly exponential growth in time. Needless to mention, a possibility cannot be ruled out that $P_\infty(t)$ becomes singular at a time later than what is covered by the present calculations. As expected, the temperature gradient grows more intensely than the passive scalar gradient does in L^2, that is, $P_1(t)$ is larger than $P_0(t)$. It should be noted that the curves $P_1(t)$, $P_2(t)$, $P_3(t)$, $P_\infty(t)$ are close to each other. Actually, $P_2(t)$ is smaller than $P_1(t)$ and it is $P_\infty(t)$ that is the smallest of this group. This means that growth of passive scalar gradient of the coupled Euler equations is not always intensified with increasing iteration number. This suggests that the Boussinesq flows are no more singular than the coupled Euler flows.

We know that it is the maximum norm of $|\nabla\theta|$ that controls regularity or singularity of solutions of the Boussinesq equations. The possibility that the above norm $P_\infty(t)$, which essentially corresponds to H_1-norm, remains finite at a blowup cannot be ruled out mathematically. In this sense $P_\infty(t)$, despite its physical meaning (as a rate of dissipation of $\langle\theta^2\rangle$ in slightly viscous cases), may not be particularly suited for detecting singularity. Rather, it is H_3-norm that becomes unbounded at a putative singularity. We are led to consider the following quantities which involve higher spatial derivatives

$$S_n(t) = \frac{1}{2}\left\langle |D^3\theta^n|^2 \right\rangle,$$

where $D \equiv (-\triangle)^{1/2}$ can be defined through Fourier transforms.[2] The Sobolev

[2]In practice, it is easier to monitor this norm than to trace a structure associated with the maximum of $|\nabla\theta|$.

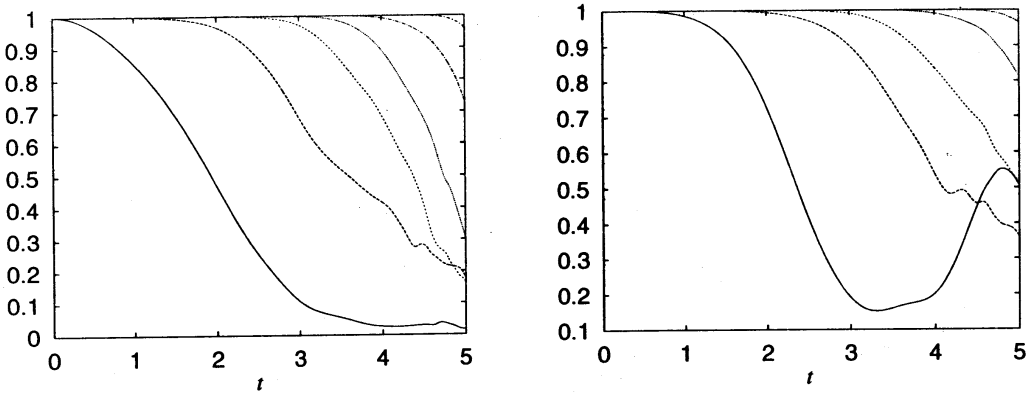

(a) (b)

Fig.3 (a) Time evolution of the correlation coefficient $C(\theta^n, \theta^\infty)$ for $n = 0$(solid), 1(dashed), 2(short-dashed), 3(dotted), 4(dash-dotted) and 5(short-dash-dotted), from left to right. (b) That of $C(\omega^n, \omega^\infty)$, depicted similarly.

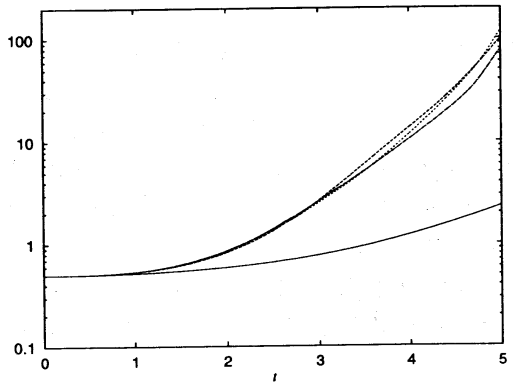

Fig.4(a) Time evolution of $P_n(t)$ for $n = 0$(solid), 1(dashed), 2(short-dashed), 5(dotted) and ∞(dash-dotted). The Euler case $n = 0$ is significantly smaller than others.

lemma

$$\max_{\boldsymbol{x}} |\nabla\theta(\boldsymbol{x}, t)| \leq C \left\langle |D^3\theta(\boldsymbol{x}, t)|^2 \right\rangle^{1/2}$$

ensures that $S_\infty(t)$ becomes unbounded simultaneously if the temperature gradient does so.

The time evolution of $S_n(t)$ for $n = 0, 1, 2, 5$ and ∞ is shown in Fig.4(b). As in the case of $P_n(t)$, $S_1(t)$ is larger than $S_0(t)$, but $S_\infty(t)$ is smaller than any of $S_1(t)$, $S_2(t), \ldots, S_5(t)$. In particular we have

$$\left\langle |D^3\theta^\infty(\boldsymbol{x}, t)|^2 \right\rangle < \left\langle |D^3\theta^1(\boldsymbol{x}, t)|^2 \right\rangle, \tag{18}$$

as far as the numerical solutions are regarded as well resolved.

Because $S_1(t)$ never become unbounded in finite time, this result indicates that the solution of the Boussinesq equations starting from IC1 shows no trend of tending to finite time blowup. In other words, unless (18) is reversed at later time, finite time blowup cannot occur. To make the point more clearly, we confider the following ratios

$$R_n(t) = \frac{\langle |D^3\theta^n|^2 \rangle}{\langle |D^3\theta^\infty|^2 \rangle}.$$

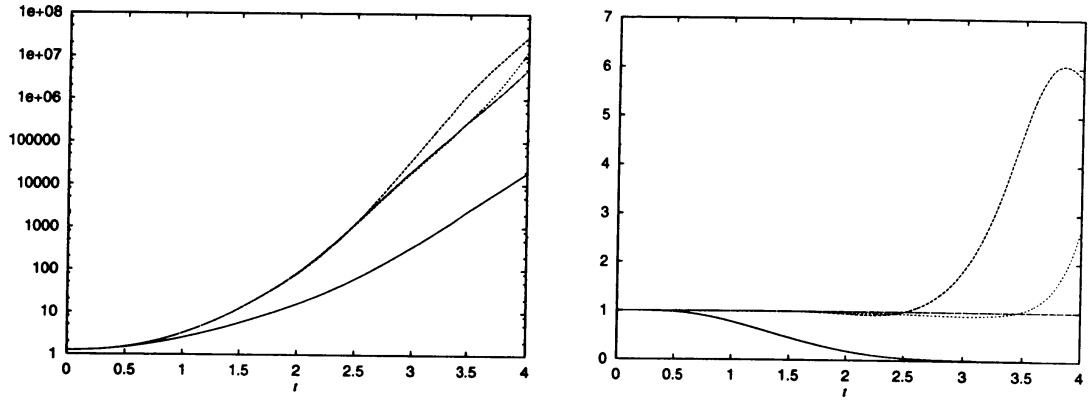

(b) (c)

Fig.4 (b) Time evolution of $S_n(t)$ for $n = 0$(solid), 1(dashed), 2(short-dashed), 5(dotted) and ∞(dash-dotted). (c) Time evolution of $R_n(t)$ for $n = 0$(solid), 1(dashed), 2(short-dashed), 5(dotted) and 10(dash-dotted).

If there is blowup at finite time, $R_n(t)$ must tend to 0, since the denominator becomes unbounded while the numerator remains finite. In Fig.4(c) we show the time evolution of $R_n(t)$ for $n = 0, 1, 2, 5$ and 10. At late times only $R_0(t)$ converges to 0, but $R_1(t)$ and $R_2(t)$ stay significantly above 1. It should be noted $R_5(t)$ is close to 1. This confirms again that at $n = 5$, the coupled Euler equations approximates the Boussinesq equations quite nicely.

In order to examine the convergence of the iteration scheme in more detail, in Fig.5(a) we show the time evolution of the complement of the normalized correlation coefficient, defined by

$$1 - C(\theta^n, \theta^\infty) \tag{19}$$

as a log-linear plot for $n = 0, 1, 2, \ldots, 10$. From this we see how correlation survives longer with the increasing iteration numbers.

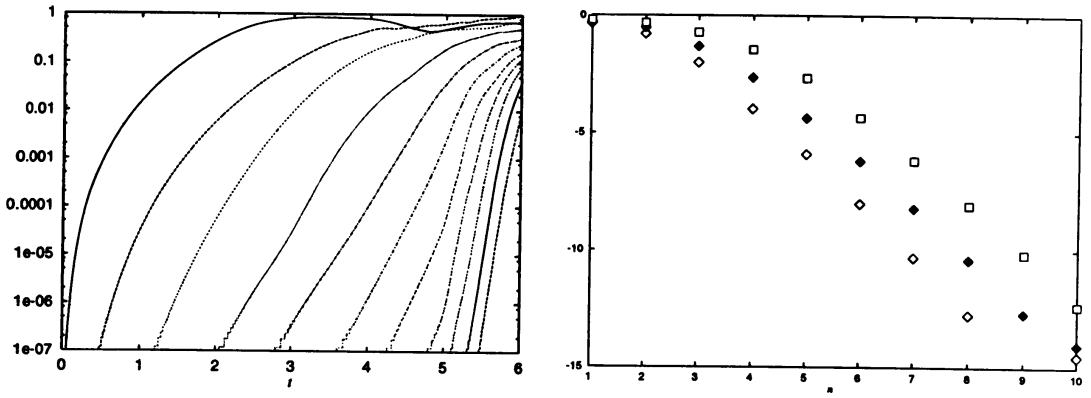

(a) (b)

Fig.5 (a) Time evolution of $1 - C(\theta^n, \theta^\infty)$ in a log-linear plot, for $n = 0,\ 1,\ 2, \ldots, 10$ from left to right. (b) Log-linear plots of $1 - C(\theta^n, \theta^\infty)$ against n at times $t = 4$(diamonds), 4.5(solid diamonds) and 5(squares).

To check the functional dependence of $1 - C(\theta^n, \theta^\infty)$ on n at fixed times, we show $1 - C(\theta^n, \theta^\infty)$ in Fig.5(b) against n at times $t = 4.0, 4.5$ and 5.0. This suggests that convergence is exponential with respect to n, that is,

$$1 - C(\theta^n, \theta^\infty) \propto \exp(-a(t)n)$$

for some positive function $a(t) > 0$ which decreases with t.

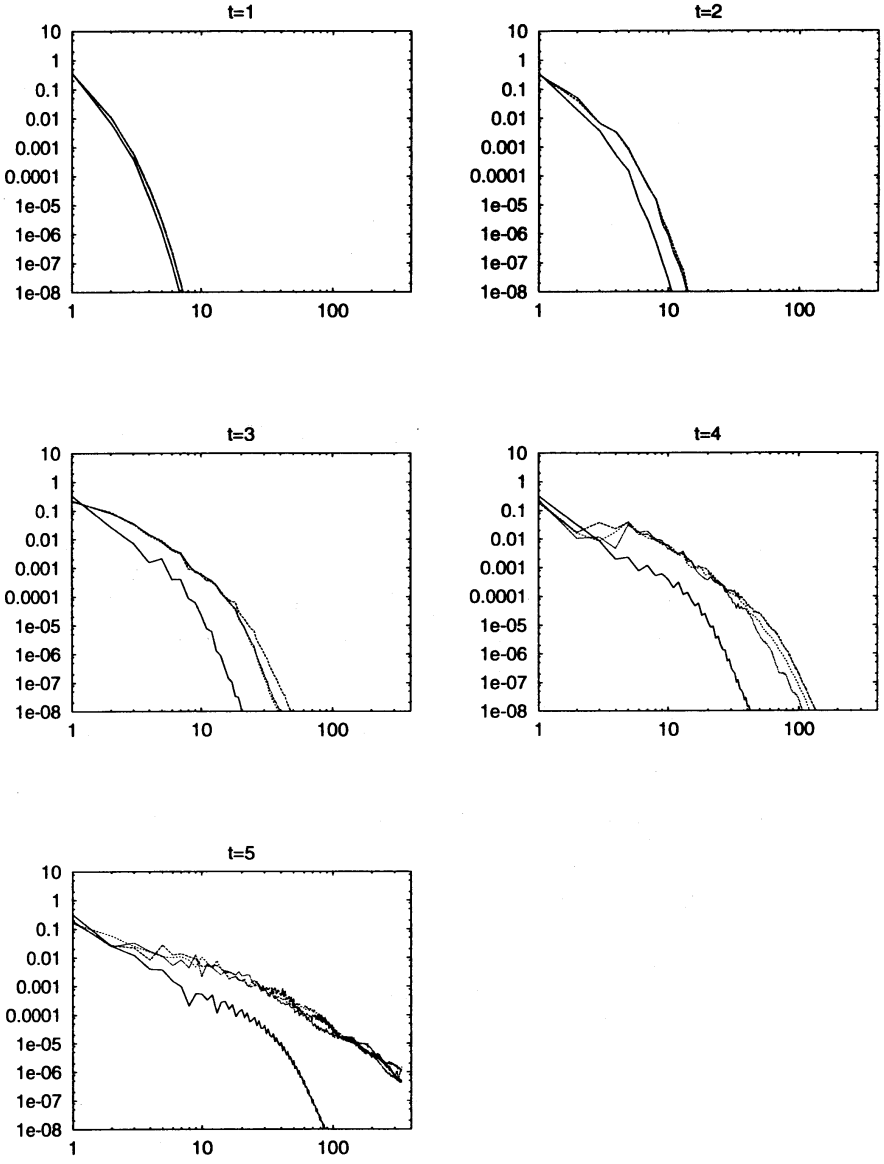

Fig.6 Time evolution of the Fourier spectra of the temperature for the Euler case $n = 0$(solid), 1(dashed), 2(short-dashed) and the Boussinesq case $n = \infty$(dotted).

To monitor how the higher wave number components are resolved it is useful to monitor the Fourier spectra of temperature defined by

$$Q(k) = \sum_{k \le |\boldsymbol{k}| < k+1} |\tilde{\theta}^n(\boldsymbol{k})|^2,$$

where $\tilde{\theta}^n(\boldsymbol{k})$ is the Fourier transform of $\theta^n(\boldsymbol{x})$. We show their time evolution for $n = 0, 1, 2, 4$ and ∞ in Fig.6. We see that the Euler flow is the most regular of all and that the coupled Euler flows and the Boussinesq flows are comparable in excitation at higher wavenumber components. All in all, we have found that the solution of the Boussinesq equations for IC1 shows no hint of going singular in finite

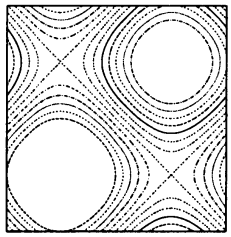

Fig.7: Contours of vorticity of IC2 $[0, 2\pi]^2$. The thresholds are $\omega = -1.4, -1.2, -1.0, \ldots 1.4$.

Now we turn our attention to the second initial condition IC2 to see whether the case of IC1 is accidental or not. The initial condition IC2 is given by

$$\text{IC2} \qquad \omega(\boldsymbol{x}, 0) = \theta(\boldsymbol{x}, 0) = \sin x + \cos y, \tag{20}$$

which is shown in Fig.7. It is a stationary solution of the usual Euler equations but is not a stationary solution of the Boussinesq equation. Therefore we can see the difference between the two equations by examining the solution starting from IC2.

We show in Fig.8 the time evolution of $P_n(t)$ for $n = 2, 5, 10$ and ∞.

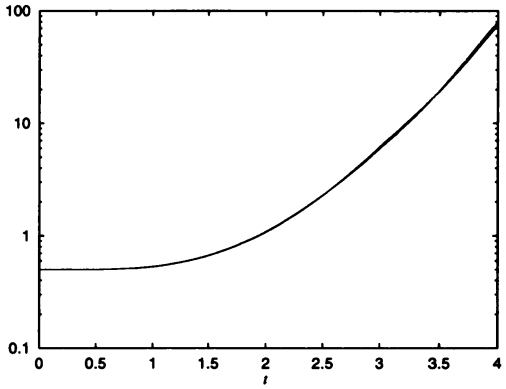

Fig.8: $P_n(t)$ for IC2; $n = 2$ (solid), 5(dashed), 10(short-dashed) and the Boussinesq case $n = \infty$(dotted). The Euler case ($n = 0$) is omitted, because it is a constant.

Because IC2 is a stationary solution, ω^0 and θ^0 has non zero Fourier component only at the smallest wavenumber, that is wavenumber 1. Also, ω^1 has excitation only at the smallest wavenumber. For $n \geq 2$, it is remarkable that they virtually collapse on each other. This suggests the iteration scheme converges quite rapidly with n for IC2 as well.

We show the time evolution of contour plots of passive scalar at $n = 5$ in Fig.9(a). For comparison, similar plots of the temperature ($n = \infty$) are shown in Fig.9(b).

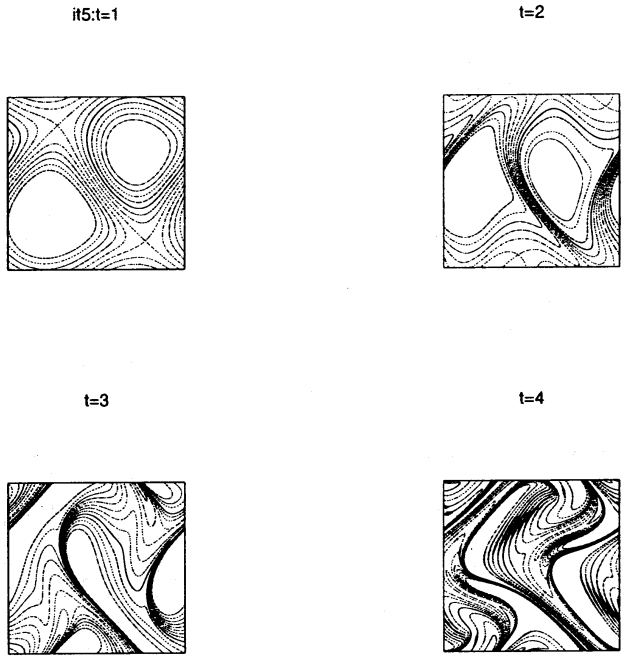

Fig.9(a): Time evolution of contour of the temperature for $n = 5$(the coupled Euler case), depicted as in Fig.8

It is impossible to distinguish these contour plots at corresponding times, which substantiates the rapid convergence of the iteration scheme. In the case of IC2, the coupled Euler equations at $n = 5$ reproduce solutions of the Boussinesq equations fairly well.

4 Theoretical considerations

4.1 Difficulty in showing convergence of the iterations

At present, it is not possible to prove that a pair of solutions (ω^N, θ^N) of (14)-(16) has a limit as $N \to \infty$. It is nevertheless useful to point out the cause of the difficulty more specifically. As mentioned above, for fixed N the system (ω^N, θ^N) has a regular solution for all time. This means that their values together with their higher derivatives of any order remain finite all the time. Therefore, for example, $||\omega^N||_\infty$ $||\nabla\theta^N||_\infty$ (or, with other suitable norms) are bounded from above on any time interval $[0, T]$. If these bounds are shown to be uniform in N, then it is possible to argue that there exists a pair of convergent subsequences $(\omega^\infty, \theta^\infty)$ on $[0, T]$, to obtain a solution to the Boussinesq equations (see for example [2] and references cited therein). According to the numerical experiments the norms used appear to be uniformly bounded in N (see, Fig.4(a) & (b) and Fig.8). Unfortunately, so far we have not been able to prove such uniform boundedness by working directly with the equations of motion.

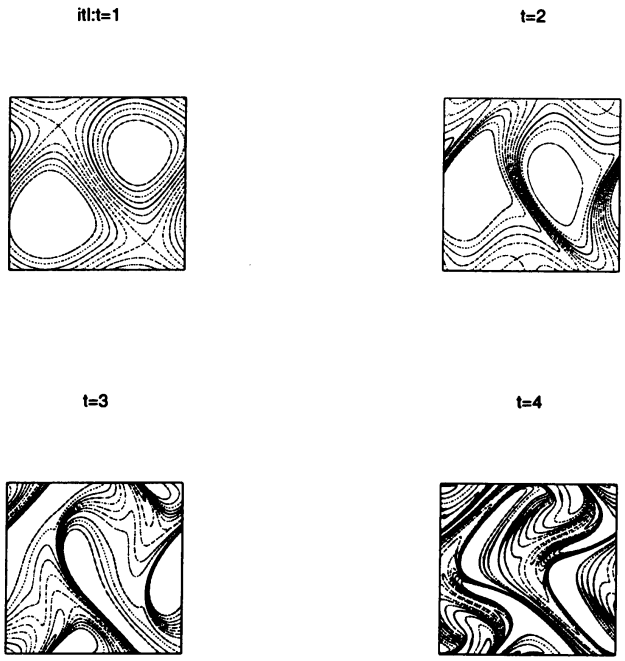

Fig.9(b): Time evolution of contour of the temperature for $n = \infty$ (the Boussinesq case), depicted similarly.

4.2 A note on a result of Cordoba and Fefferman

The numerical results presented in the previous section suggests regularity of the solutions of the Boussinesq equations rather than their singularity. As mentioned in Introduction, global regularity of the Boussinesq has not yet been demonstrated. Nevertheless there are some mathematical results that restrict possible formation of singularity. One recent result [18] claims that if a singularity is formed in finite time by coalescence of level sets of θ, then not only $\nabla\theta$ but also the velocity must become unbounded at that time. Their result is valid for any active scalar equations. Here we consider the what this result means in the particular case of the Boussinesq equations.

Retaining the integral representation (3) we may rewrite (6) as

$$\frac{\partial \boldsymbol{u}}{\partial t} + (\boldsymbol{u}\cdot\nabla)\boldsymbol{u} = -\nabla p + \begin{pmatrix} R_1 R_2[\theta] \\ R_2 R_2[\theta] + \theta \end{pmatrix}, \tag{21}$$

where $R_i = (-\triangle)^{-1/2}\partial_i$ is the Riesz transform. The second term on the right-hand side of (21) is not bounded by a constant, but it satisfies the following inequality [19, 20]

$$||R_i R_j[\theta]||_\infty \leq C||\theta||_\infty \left[1 + \log_+\left(L\frac{||\nabla\theta||_\infty}{||\theta||_\infty}\right)\right]$$

where $i, j = 1$ or 2, $\log_+ x = \max(\log x, 0)$ and

$$C(>0),\ L=\sqrt{\frac{||\theta||_1}{||\theta||_\infty}}$$

are constants.

Suppose that we attempt to reconstruct the velocity of the Boussinesq equations by solving forced Euler equations with an appropriate external force

$$\frac{\partial \boldsymbol{u}}{\partial t}=-\{(\boldsymbol{u}\cdot\nabla)\boldsymbol{u}\}^{\mathrm{tr}}+\boldsymbol{f}, \tag{22}$$

where we have put $\{(\boldsymbol{u}\cdot\nabla)\boldsymbol{u}\}^{\mathrm{tr}}\equiv(\boldsymbol{u}\cdot\nabla)\boldsymbol{u}+\nabla p$. Given $\theta(\boldsymbol{x},t)$, we can choose the forcing term *a posteori* as

$$\boldsymbol{f}=\begin{pmatrix} R_1R_2[\theta] \\ R_2R_2[\theta]+\theta \end{pmatrix}.$$

If a singularity is formed by coalescence of level sets of θ, by a theorem [18] we have $||\boldsymbol{u}||_\infty=\mathcal{O}((t_*-t)^{-n})$ with $n\geq 1$ or

$$\left|\left|\frac{\partial \boldsymbol{u}}{\partial t}\right|\right|_\infty=\mathcal{O}((t_*-t)^{-(n+1)}).$$

On the other hand we have by [6, 7] $||\nabla\theta||_\infty$ must diverge at least as $(t_*-t)^{-2}$ for a possible blowup. Assuming an algebraic blow-up[3]

$$||\nabla\theta||_\infty=\mathcal{O}((t_*-t)^{-m}),\ \text{with}\ \ m\geq 2,$$

the forcing term is bounded as follows

$$||\boldsymbol{f}||_\infty\leq C\log\left(\frac{1}{t_*-t}\right),$$

with a positive constant C. Then, $\dfrac{\partial \boldsymbol{u}}{\partial t}$ must be balanced with $\{(\boldsymbol{u}\cdot\nabla)\boldsymbol{u}\}^{\mathrm{tr}}$. This is a contradiction, since as $t\to t_*$, the forcing term becomes negligible and the forced Euler equations become unforced in the limit $t\to t_*$. It is impossible for the Boussinesq equations to go singular by the mechanism of coalescence of level sets of θ associated with algebraically singular $||\nabla\theta||_\infty$.

5 Summary and discussion

We have proposed a successive approximation scheme that generates a solution of the Boussinesq equations on the basis of solutions two-dimensional Euler equations.

If $(\boldsymbol{u}^N,\theta^N)$ has a limit in some sense as $N\to\infty$, that is, the system (14)-(16) has a kind of 'fixed-point property', it solves the Boussinesq equations. Whether the Boussinesq equations remain regular for all time or not depends on the convergence of the iteration scheme. Because such convergence is not obvious mathematically we have performed some numerical experiments using a pseudo-spectral method.

[3]Much stronger singularities, e.g. $\exp(t_*-t)^{-n}$ $(n>0)$, cannot be ruled out. But such a behavior has not been reported to occur in numerical experiments.

The iteration scheme turned out to converge rapidly as far as the current numerical results are concerned, suggesting global regularity of the Boussinesq equations.

On the other hand, if a solution to the Boussinesq equations goes singular at some later time which cannot be covered at the present resolutions, then convergence of a solution of the coupled Euler equations to that of the Boussinesq equations must be invalidated by the time of blowup. Therefore, numerical experiments supporting blowup for the Boussinesq equations should observe a behavior in $\nabla\theta$ markedly different from a corresponding quantity of the coupled Euler equations. In this sense, the present method will serve as a solid criterion for monitoring singularity formation in the Boussinesq equations.

In place of (14)-(16) we may consider yet another method of successive approximations

$$\frac{\partial \omega^n}{\partial t} + (\boldsymbol{u}^{n-1} \cdot \nabla)\omega^n = \frac{\partial \theta^{n-1}}{\partial x_1}, \tag{23}$$

$$\frac{\partial \theta^n}{\partial t} + (\boldsymbol{u}^{n-1} \cdot \nabla)\theta^n = 0, \tag{24}$$

$$\nabla \cdot \boldsymbol{u}^0 = \nabla \cdot \boldsymbol{u}^n = 0, \tag{25}$$

which is a straightforward generalization of Kato's idea [1]. Note that they are linear with respect to ω^n and θ^n, respectively. We can prove local existence for the Boussinesq equations by repeating the arguments used in [1]. However we do not know if it is possible to extend the time interval of local existence, because of lack of vorticity conservation, as pointed out to the author by Prof. H. Okamoto.

Acknowledgments

The author would like to thank Professor H. Okamoto and Dr. M. Iima for useful comments.

This work has been partially supported by Grant-in-Aid for scientific research from the Ministry of Education, Culture, Sports, Science and Technology of Japan, under Nos. 11304005 and 11214204.

6 Appendices ([21],[22])

6.1 Conserved quantities

There are obvious conservation laws to (6)

$$\int_{\mathbb{R}^2 \text{ or } \mathbb{T}^2} F_1(\theta(\boldsymbol{x}))d\boldsymbol{x}, \tag{26}$$

where the domain of integration extends over $\mathbb{R}^2$ (infinite plane) or in $\mathbb{T}^2$ (for periodic boundary conditions). Moreover, (6) conserves

$$\int_{\mathbb{R}^2} \left(\frac{|\boldsymbol{u}|^2}{2} - y\theta \right) d\boldsymbol{x} \tag{27}$$

for the infinite plane case and

$$\int_{\mathbb{T}^2} \left(\frac{|\boldsymbol{u}|^2}{2} - (y-b)\theta \right) d\boldsymbol{a} \tag{28}$$

under periodic boundary conditions, where (a, b) is a set of Lagrangian marker variables such that $(a, b) = (x, y)$ at $t = 0$.

6.2 Stationary solutions

It is well-known that stationary solutions of two-dimensional Euler equations are characterized by a family of one arbitrary function relating vorticity ω and stream function ψ. In contrast, it requires two arbitrary functions to specify stationary solutions of two-dimensional Boussinesq equations, say F and G.

In $\mathbb{R}^2$, stationary solutions of (8,9) have the following representation

$$\theta = F(\psi), \tag{29}$$

$$\omega + F'(\psi)y = G(\psi). \tag{30}$$

The second relation is derived as follows

$$\frac{\partial(\omega,\psi)}{\partial(x,y)} = F'(\psi)\frac{\partial(\psi,y)}{\partial(x,y)} = \frac{\partial(\psi,F'(\psi)y)}{\partial(x,y)}. \tag{31}$$

In $\mathbb{T}^2$ such an representation is not valid.

6.3 Analogy with three-dimensional axisymmetric flows

In the axisymmetric case $\frac{\partial}{\partial\phi} = 0$, the three-dimensional Euler equations can be written in cylindrical coordinates (r,ϕ,z) as

$$\left(\frac{\partial}{\partial t} + \boldsymbol{u}\cdot\nabla\right)\boldsymbol{u} = \frac{1}{r^3}(ru_\phi)^2\boldsymbol{e}_r - \nabla p,$$

$$\left(\frac{\partial}{\partial t} + \boldsymbol{u}\cdot\nabla\right)(ru_\phi) = 0,$$

and

$$\left(\frac{\partial}{\partial t} + \boldsymbol{u}\cdot\nabla\right)\frac{\omega_\phi}{r} = \frac{1}{r^4}\frac{\partial}{\partial z}(ru_\phi)^2,$$

where $\boldsymbol{u} = (u_r, u_\phi, u_z)$.

If we accept the following correspondence

$$ru_\phi \Longleftrightarrow \theta,$$

$$\frac{\omega_\phi}{r} \Longleftrightarrow \omega,$$

then the three-dimensional axisymmetric equations are similar to the two-dimensional Boussinesq equations (except at $r = 0$). The work [10] regarding the three-dimensional axisymmetric Euler equations is based on this analogy.

References

[1] Kato, T.(1964). On classical solutions of the two-dimensional non-stationary Euler equation, *Arch. Rat. Mech. Anal.*, **25**, 302.

[2] Sulem, C. and Sulem, P.-L. (1983). The well-posedness of the two-dimensional ideal flow, *J. Méc. Théor. Appliqu.*(Paris) Special issue on two-dimensional turbulence, **42**, 217.

[3] Wolibner, W.(1933). Un theorém sur l'existence du mouvement plan d'un fluide parfait, homogéne, incompressible, pendant un temps infiniment long, *Math. Z.*, **37**, 698.

[4] Schaeffer, A.C. (1937). Existence theorem for the flow of an ideal incompressible fluid in two dimensions, *Trans. of the A.M.S.*, **42**, 497.

[5] Kato, T. (2001). A remark on the 2D-Euler equations, unpublished manuscript contained in this volume.

[6] E, W. and Shu, Ch.-W.(1994). Small-scale structures in Boussinesq convection, *Phys. Fluids*, **6**, 49.

[7] Chae, D. and Nam, H.-S.(1997). Local existence and blow-up criterion for the Boussinesq equations, *Proc. Roy. Soc. Edinburgh* Sect. A **127**, 935.

[8] Beale, J.T., Kato, T and Majda A.(1984). Remarks on the breakdown of smooth solutions for the 3D Euler equations, *Comm. Math. Phys.*, **94**, 61.

[9] Grabowski, W.W. and Clark, T.L.(1991). Cloud-environment interface instability: rising thermal calculations in two spatial dimensions, *J. Atoms. Sci.*, **48**, 527.

[10] Pumir, A. and Siggia, E.D.(1992). Development of singular solutions to the axisymmetric Euler equations, *Phys. Fluids* A, **4**, 1772.

[11] Pumir, A., Shraiman, B.I. and Siggia, E.D.(1992). Vortex morphology and Kelvin's theorem, *Phys. Rev.* A, **45**, R5351.

[12] Grauer, R. and Sideris, T.C.(1995). Finite time singularities in ideal fluids with swirl, *Physica* D, **88**, 116.

[13] Carmack, L.A.(1997). Vorticity amplification in incompressible ideal swirling flow without a boundary, *Phys. Fluids*, **9**, 1379.

[14] Toh, S., Matsumoto T., Miyashita H. and Yamada, Y.(2001) Intermittency and singularity in an active scalar turbulence - *finite time singularity in the two-dimensional ideal Boussinesq approximation equations*- (in Japanese), *Reports of RIAM Symposium*, **No.12ME-S1**, 20.

[15] Majda, A.J. and Tabak, E.G.(1996). A two-dimensional model for quasi-geostrophic flow: comparison with the two-dimensional Euler flow. *Physica D*, **98**, 515.

[16] Constantin, P., Majda, A.J. and Tabak, E.(1994). Formation of strong fronts in the 2-D quasigeostrophic thermal active scalar, *Nonlinearity*, **7**, 1495.

[17] Ohkitani, K. and Yamada,M.(1997). Inviscid and inviscid-limit behavior of a surface quasi-geostrophic flow, *Phys. Fluids*, **9**, 876.

[18] Cordoba, D. and Fefferman, C.(2001). Scalars convected by a 2D incompressible flow, *Commun. Pure Appl. Math.*, **54**, 1.

[19] Constantin, P. and Wu, J.(1996). The inviscid limit for non-smooth vorticity *Indiana. Univ. Math. J.*, **45**, 67.

[20] Constantin, P.(1998). Absence of proper nondegenerate generalized self-similar singularities, *J. Stat. Phys.*, **93**, 777.

[21] Abarbanel, H.D., Holm, D.D., Marsden, J.E. and Ratiu, T.S.(1986). Nonlinear stability analysis of stratified fluid equilibria, *Phil. Trans. R. Soc. Lond.* A, **318**, 349.

[22] Szeri A. and Holmes, P.(1988). Nonlinear stability of axisymmetric swirling flows, *Phil. Trans. R. Soc. Lond.* A, **326**, 327.